

Title	A Proton Conductive Porous Framework of an 18-Crown-6-Ether Derivative Networked by Rigid Hydrogen Bonding Modules
Author(s)	Chen, Xin; Huang, Rui Kang; Takahashi, Kiyonori et al.
Citation	Angewandte Chemie - International Edition. 2022, 61(45), p. e202211686
Version Type	AM
URL	https://hdl.handle.net/11094/92731
rights	© 2022 Wiley-VCH Verlag GmbH & Co. KGaA.
Note	

Osaka University Knowledge Archive : OUKA

<https://ir.library.osaka-u.ac.jp/>

Osaka University

A Proton Conductive Porous Framework of an 18-Crown-6-Ether Derivative Networked by Rigid Hydrogen Bonding Modules

Xin Chen,^[a] Rui-Kang Huang,^[a,b] Kiyonori Takahashi,^[a,b] Shin-ichiro Noro,^[c] Takayoshi Nakamura,^{*,[a,b]} and Ichiro Hisaki^{*,[a,b,d]}

[a] Dr. X. Chen, Dr. R.-K. Huang, Dr. K. Takahashi, Prof. Dr. T. Nakamura, Prof. Dr. I. Hisaki
Graduate School of Environmental Science,
Hokkaido University,
Sapporo, Hokkaido 060-0810, Japan

[b] Dr. R.-K. Huang, Dr. K. Takahashi, Prof. Dr. T. Nakamura, Prof. Dr. I. Hisaki
Research Institute for Electronic Science,
Hokkaido University,
Sapporo, Hokkaido 001-0020, Japan
Email: tnaka@es.hokudai.ac.jp (T.N.)

[c] Prof. Dr. S. Noro
Faculty of Environmental Earth Science,
Hokkaido University,
Sapporo, Hokkaido 060-0810, Japan

[d] Prof. Dr. I. Hisaki
Division of Chemistry, Graduate School of Engineering Science,
Osaka University,
1-3 Machikaneyama, Toyonaka, Osaka 560-8531, Japan
Email: i.hisaki.es@osaka-u.ac.jp (I.H)

Supporting information for this article is given via a link at the end of the document.

Abstract: A rigid hydrogen-bonded organic framework (HOF) was constructed from a C_3 -symmetric hexatopic carboxylic acid with a hydrophilic 18-crown-6-ether (18C6) component. Despite the flexible macrocyclic structure with many conformations, the derivative with three dicarboxy-*o*-terphenyl moieties in the periphery yielded a rigid layered porous framework through directional intermolecular hydrogen bonding. Interestingly, the HOF possesses 1D channels with bottleneck composed of 18C6 rings. The HOF shows proton conductivity ($1.12 \times 10^{-7} \text{ S cm}^{-1}$) through Grotthuss mechanism ($E_a = 0.27 \text{ eV}$) under 98%RH. The present unique water channel structure provides an inspiration to create molecular porous materials.

Since it was reported by Pedersen in 1967,^[1] crown ethers including [18]crown-6-ether (18C6) have been one of the most important ionophores and building block molecules in host-guest and supramolecular chemistry because of its highly-selective recognition ability toward specific cationic and molecular species.^[2] Particularly, crystalline porous frameworks composed of crown ether building blocks are promising candidates for functional materials, because crown ether moieties can ideally be arranged with precise periodicity and orientation, and furthermore, guest molecules or analytes are capable of accessing to the crown ether through the channel spaces. A handful of metal-organic frameworks (MOFs)^[3] and covalent organic frameworks (COFs)^[4] composed of crown ether building blocks were reported. For example, Shu and coworkers demonstrated that the MOFs incorporating dibenzo18C6 showed the improved hydrogen uptake depending on cations inserted in the crown ether moiety.^[3b] However, such frameworks are very limited because of a highly flexible crown

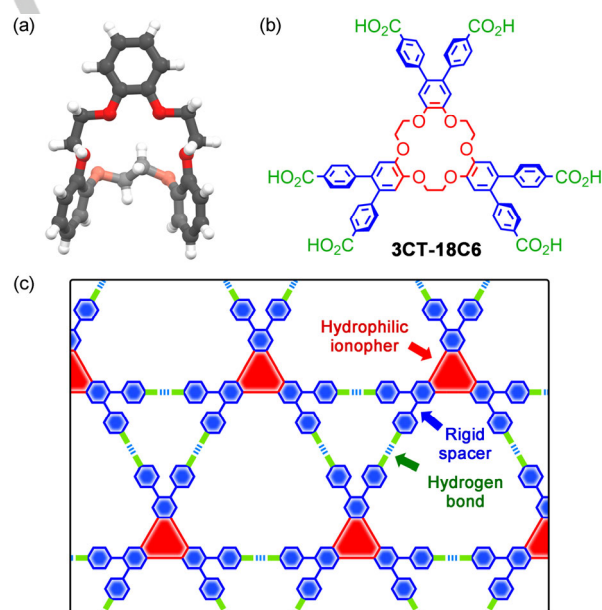


Figure 1. (a) Nonplanar conformation of pristine T18C6 in solid state. (b) Chemical structure of 3CT-18C6. (c) Expected H-bonded porous network composed of 3CT-18C6.

ether skeletons with various low-symmetric conformations.^[5] Particularly, there is no example of crown ether-based porous hydrogen-bonded organic frameworks (HOFs),^[6] although reversible H-bonds in HOFs can usually provide highly-crystalline porous frameworks.

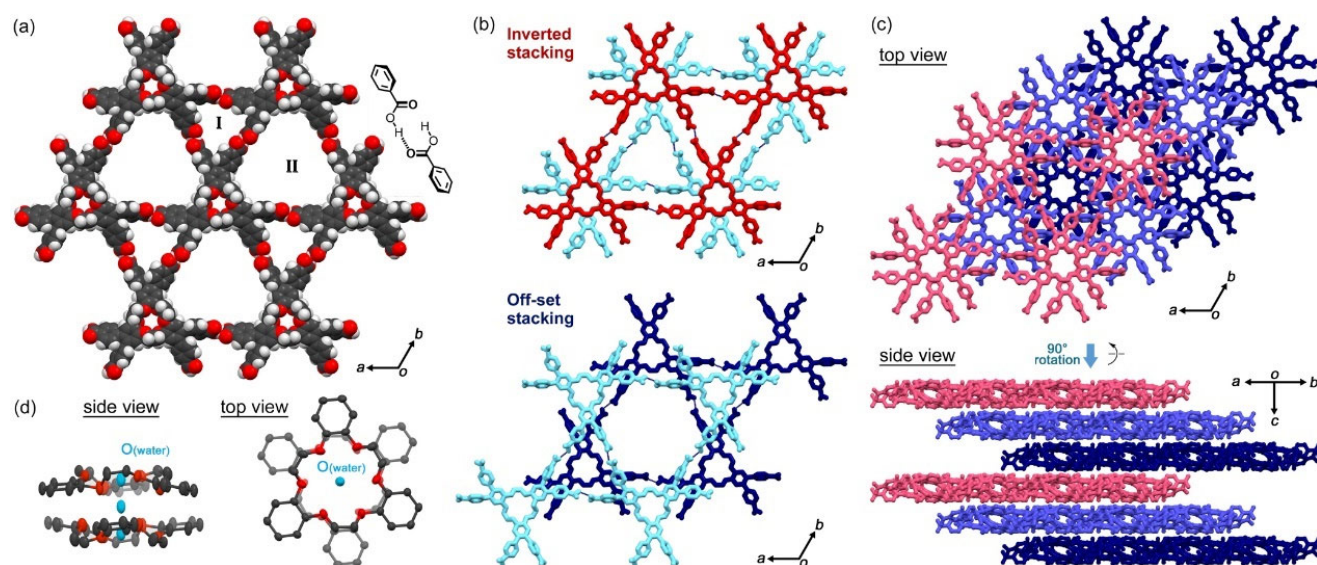


Figure 2. Crystal structure of HOF **3CT-18C6-I**. a) H-bonded HexNet sheet with two kinds of voids I and II, where the carboxy groups make mono-connected dimer. (b) Stacking manner of the HexNets sheets: (top) inverted stacking in which the 18C6 moieties are overlapped, (bottom) off-set stacking in which void II is covered by 18C6 moiety. (c) Packing diagram in which the bilayer formed through inverted stacking of the HexNet is colored in pink, purple, or dark blue. (d) Water molecules disordered in the dimer of 18C6, in which peripheral carboxyphenyl groups are omitted for clarity.

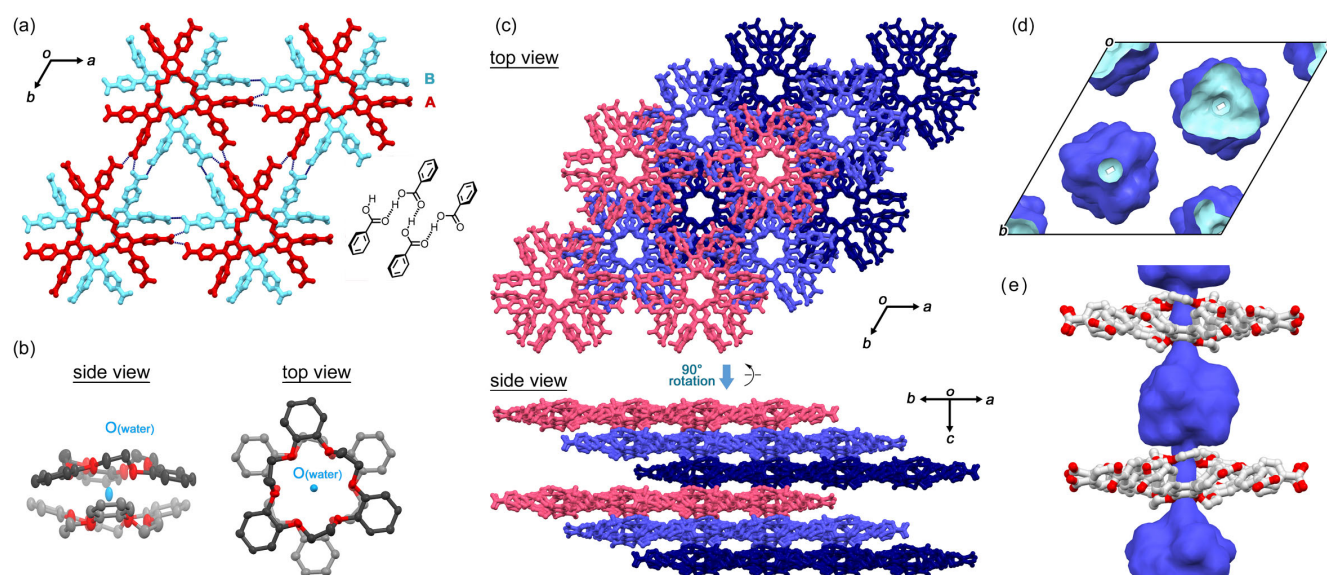


Figure 3. Crystal structure of activated HOF **3CT-18C6-Ia**. a) H-bonded HexNet bilayer, where the carboxy groups make interlayer H-bonds to give truncated tetramer. (b) Water molecules remained in the dimer of 18C6, in which peripheral carboxyphenyl groups are omitted for clarity. (c) Packing diagram in which the bilayer formed through inverted stacking of the HexNet is colored in pink, purple, or dark blue. (d) Visualized solvent accessible surface, where purple and sky blue indicate outside and inside of the void. (e) 1D channel with bottle neck of the dimeric 18C6 moiety.

In this study, we newly designed 18C6 derivative with three 4,4'-dicarboxy-*o*-terphenyl (CT) groups (**3CT-18C6**) as shown in Figure 1. Although pristine tribenzo18C6 exhibits a non-planar conformation in crystalline states (Figure 1a),^[7] we expected that incorporation of three CT groups in 18C6 provides a crystalline HOF with permanent porosity by a rigid spacer and highly-directional and predictable H-bonding between the carboxy groups (Figure 1b,c).^[8] Herein, we demonstrate that **3CT-18C6** forms a C_3 -symmetric rigid crystalline HOF **3CT-18C6-I**. This is the first example of a rigid HOF with permanent porosity composed of flexible crown ether derivatives, although non-porous framework based on 18C6 was reported.^[9] Interestingly, the HOF has one-dimensional (1D) channels with a shish kebab-

like shape with the bottleneck part composed of eclipse-stacked 18C6 macrocycles. The HOF shows proton conductivity through Grotthuss mechanism under 98%RH. This HOF can provide fundamental insight of the proton conducting pass through the narrow 18C6 channel.

3CT18C6 was synthesized from tribenzo18C6 (for details, see SI) and recrystallized by slow evaporation using a mixed solution of *N,N*-dimethylformamide (DMF), H₂O, ethanol and 2M HCl (*v/v* = 2/0.5/0.3/0.05) at 80 °C, afforded a HOF **3CT18C6-I** as colourless crystals. Single crystal X-ray diffraction (SCXRD) analysis revealed that **3CT-18C6** crystallizes in trigonal space group $R\bar{3}$ to give **3CT18C6-I** possessing a hexagonal network (HexNet) structure (Figure 2, Table S1).^[10] The molecule has

three-fold axis at the centre of the macrocycle. The oxygen and sp^3 -carbon atoms in the macrocycle are disordered in two positions with an occupancy of 0.56 : 0.44 (Figure S1). The molecules are connected through a twisted single H-bond between the carboxy groups with a $O\cdots O$ distance of 2.60 Å and a dihedral angle of ca. 67.2° to form a 2D HexNet sheet (Figure 2a). The 2D networks are stacked in two ways (Figure 2b): (1) an inverted stacking fashion with a mean interlayer distance of 3.90 Å so as the 18C6 moieties to be overlapped with an equipped manner and (2) an offset stacking fashion with interlayer distance of 3.81 Å. The layers are stacked without interpenetration to give layered HOF **3CT-18C6-I** (Figure 2c) with shish-kebab shaped 1D channels accommodating solvent guest molecules (Figure S2). It is noteworthy that the inverted stacking makes two molecules of **3CT-18C6** form a bottleneck of the 1D channel (Figure 2d). One water molecule is accommodated in a space of the dimerized 18C6 moiety with a disordered fashion. The peripheral phenylene groups are alternately contacted to those in the other molecule with the contact angle of 74.12° , which is typical face-to-edge interaction to stabilize the dimer (Figure S3). The potential solvent accessible void space accounts for approximately 33.7% of the whole crystal volume as estimated by PLATON.^[11] A powder X-ray diffraction (PXRD) pattern of as-synthesized HOF **3CT-18C6-I** is in good agreement with the pattern simulated from the SCXRD structure, indicating high phase purity and good stability of the HOF in bulk amount (Figure S4). Thermogravimetric (TG) analysis of the as-formed **3CT-18C6-I** and 1H NMR spectroscopy of **3CT-18C6-I** dissolved in $DMSO-d_6$ indicate that the HOF contains water and DMF molecules (Figures S5 and S6, respectively). Variable temperature PXRD experiments indicated that **3CT-18C6-I** underwent irreversible structural changes upon heating (Figure S7).

To remove included solvent molecules from the framework, as-formed HOF **3CT-18C6-I** was heating at $160^\circ C$ under a vacuum condition for 1 day. PXRD indicated that the activated material retained crystallinity (Figure S8), and moreover, SCXRD analysis successfully revealed the crystal structure of activated HOF **3CT-18C6-Ia** (Figure 3). The crystal structure of **3CT-18C6-Ia** was desymmetrized through activation: the space group was changed from $R\bar{3}$ into $R3c$, and the structure consists of crystallographically independent two molecules of **3CT-18C6** (A and B), both of which have a C_3 -axis at the centre of the 18C6 ring. The independent molecules respectively form the corresponding HexNet layers, which are stacked with the inverted manner to give a bilayer similar with the case of **3CT-18C6-I**. More detailed comparison revealed the following structural differences between **3CT-18C6-I** and **3CT-18C6-Ia**. **3CT-18C6-Ia** involves a truncated interlayer H-bonded tetramer among carboxy groups as shown in Figure 3a(inset), in instead of a single-connected H-bond. Furthermore, a stacked dimer shows different conformation of the peripheral phenylene groups (Figure S9). The phenylene groups are contacted in nearly perpendicular in **3CT-18C6-I** as described above, while the groups are contacted in nearly parallel manner with the contact angle of 14° in the case of **3CT-18C6-Ia** (Figure S3). It is not negligible that water molecules still remain in the void of **3CT-18C6-Ia** even after activated at high temperature under vacuum condition (Figure 3b), which was also supported by TG analysis (Figure S10). Particularly, one of them is located at the middle of the 18C6 dimer. The void space retains the shish-kebab shaped

1D channel. The potential solvent accessible void space accounts for 17.0% of the whole crystal volume as estimated by PLATON.^[11] The structural feature of the channel is that the bottle-neck part is composed of the hydrophilic 18C6 dimer, while the other part is of the hydrophobic CT moieties.

The HOF showed no significant N_2 adsorption at 77 K, while showed moderate CO_2 uptake ($76.5\text{ cm}^3\text{g}^{-1}$ at $P/P_0 = 0.99$) at 195 K (Figure 4a), indicating that the channel has a narrow aperture which can pass smaller CO_2 molecules with the kinetic diameter of 3.30 Å, instead of N_2 with that of 3.64 Å. A quadrupolar nature of CO_2 is also anticipated to play a role for adsorption as reported in many HOF systems. The CO_2 sorption isother shows rapid uptake at low pressure region of $P/P_0 < 0.05$, indicating existence of micro pore. The remarkable hysteric behavior is probably caused from bottlenecked 1D structure of the pore. H_2O adsorption isotherms shows nearly linear isotherms with uptake of 7 mmol g^{-1} at $P/P_0 = 0.9$ (Figure 4b). The amount of absorbed water in **3CT-18C6-Ia** is larger than that of HOF-GS-10 possessing narrow channel (3.47 mmol g^{-1}), while smaller than that of HOF-GS-11 with larger channel (11.6 mmol g^{-1}), both of which are representative protonconductive bicomponent

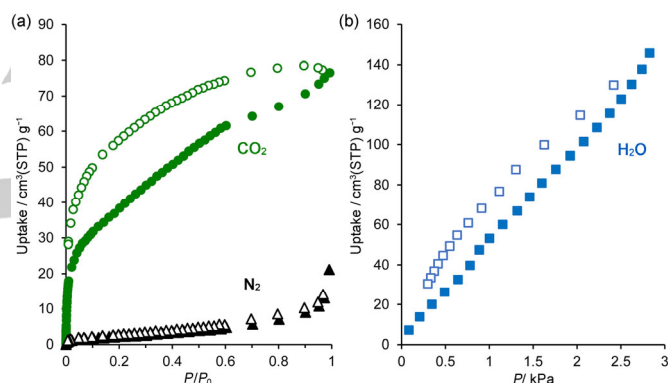


Figure 4. Sorption isotherms of **CT-18C6-Ia** for (a) N_2 at 77 K and CO_2 at 195 K and (b) water at 298 K. Open symbols: adsorption. Solid symbols: desorption.

HOFs.^[12]

Since **3CT-18C6-Ia** has the permanent pore composed of the 18C6 and shows no structural changes upon H_2O uptake (Figure S11), **3CT-18C6-Ia** was expected to exhibit proton conductivity under high relative humidity conditions. The temperature dependence of the Nyquist diagram of **3CT-18C6-Ia** in ~ 85 and $\sim 98\%$ RH is summarized in Figures S12a and 5a, respectively. The Nyquist diagrams of **3CT-18C6-Ia** at $\sim 98\%$ RH are semicircles from 24 to $65^\circ C$. The proton conductivity of **3CT-18C6-Ia** was estimated from an equivalent circuit model (for details, see Figures S12b and S12c, and Tables S2 and S3), and temperature-dependence of bulk conductivity are summarized as Arrhenius plots (Figure 5b). From the plot, the proton conductivities at $20^\circ C$ under $\sim 85\%$ RH and 98% RH were estimated to be $1.49 \times 10^{-8}\text{ S cm}^{-1}$ and $1.12 \times 10^{-7}\text{ S cm}^{-1}$, respectively. The conductivity of the present system is comparable to previously reported non-porous 18C6-based framework **2CT-18C6-III** that showed proton conductivity of 3.43 S cm^{-8} ($27^\circ C$, 85% RH),^[9] and is smaller compared with reported other HOFs,^[13] probably due to a narrow bottleneck controlled by 18C6. For example, mono-component HOFs p -

6PA-HPB,^[14] HOF-6a,^[15] and HOF-H₃L^[16] showed the conductivity of 2.5×10^{-2} (rt, 95%RH), 3.4×10^{-6} (27 °C, 97%RH), and 6.91×10^{-5} (100 °C 98%RH) S cm⁻¹, respectively. Moreover, acid-based combined multi-component HOFs showed much larger proton conductivity: 0.75×10^{-2} S cm⁻¹ for HOF-GS-10^[12] (30 °C, 95%RH), 2.2×10^{-2} S cm⁻¹ for CPOS-2^[17] (60 °C, 98%RH), 9.0×10^{-2} S cm⁻¹ for UPC-H3^[18] (80 °C, 99%RH), and 2.37×10^{-1} S cm⁻¹ for a single crystal of UPC-H9^[19] (80 °C 60%RH). The increase in proton conductivity with increasing relative humidity is the same as that observed for proton conductive HOFs.^[12] The E_a of **3CT-18C6-Ia** at ~85 and 98%RH is 0.75 and 0.27 eV, respectively. The proton conduction mechanisms at ~85 and ~98%RH are attributed to Vehicle and Grotthuss mechanisms, respectively.^[20] The efficient proton transfer pathway was constructed at high relative humidity, resulting in a higher proton conduction value, and a lower E_a consistent with the Grotthuss mechanism. This corresponds to the results of the H₂O

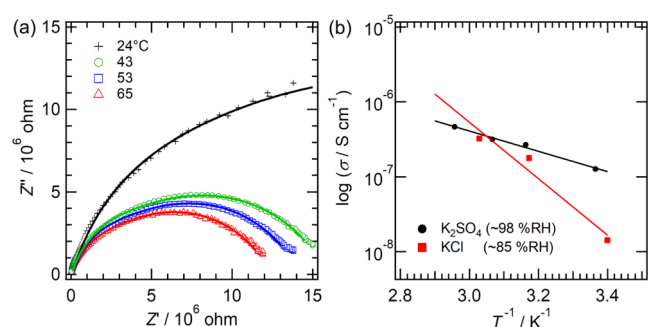


Figure 5. Proton conductivity for pellet samples of **3CT-18C6-Ia**. (a) Temperature dependence of Nyquist diagram under ~98%RH. (b) Arrhenius plot of proton conductivity calculated from impedance spectroscopy.

adsorption isotherm, where more H₂O was adsorbed at higher relative pressures.

In summary, we synthesized **3CT-18C6** and successfully constructed a C₃-symmetric rigid crystalline HOF **3CT-18C6-I**. This is the first example of a rigid, porous HOF composed of flexible crown ether derivatives. The activated HOF **3CT-18C6-Ia** has one-dimensional (1D) channels with a shish kebab like shape and the bottleneck part of the channel composed of eclipse-stacked 18C6 macrocycles. Because of the 1D channel, the HOF shows proton conductivity through Grotthuss mechanism under 98% of RH. The present HOF with unique water channel structure provides an inspiration to create molecular porous materials.

Acknowledgements

This work was supported by KAKENHI (JP19H04557, JP21K18961, JP21H01919, JP21K18961, JP21H05485), Bilateral Programs (JPJSBP120207401), and by the Dynamic Alliance for Open Innovation Bridging Human, Environment and Materials from MEXT and JSPS, Japan. I.H. thanks Hoansha Foundation and Nagase Science and Technology Foundation. X.C. thanks the Chinese Scholarship Council (CSC) for financial support. I.H. also thanks Multidisciplinary Research Laboratory

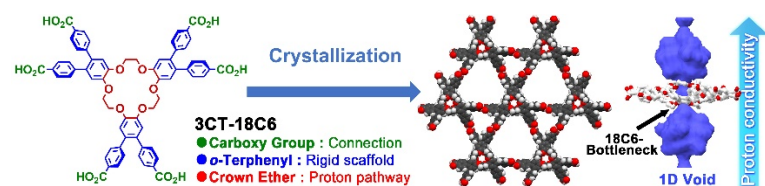
System for Future Developments (MRL), Graduate School of Engineering Science, Osaka University. The authors thank Profs. Y. Sagara (currently at Tokyo Institute of Technology) and N. Tamaoki at RIES, Hokkaido University for purification of compounds by preparative HPLC, and Ms. R. Miyake at Osaka University for HR-MS analysis.

Keywords: crown ether • hydrogen bond • porous framework • proton conduction • crystal engineering

- [1] a) C. J. Pedersen, *J. Am. Chem. Soc.* **1967**, *89*, 2495–2496; b) J. Pedersen, *J. Am. Chem. Soc.* **1967**, *89*, 7017–7036.
- [2] a) F. C. J. M. van Veggel, W. Verboom, D. N. Reinhoudt, *Chem. Rev.* **1994**, *94*, 279–299; b) F. M. Raymo, J. F. Stoddart, *Chem. Rev.* **1999**, *99*, 1643–1663; c) G. W. Gokel, W. M. Leevy, M. E. Weber, *Chem. Rev.* **2004**, *104*, 2723–2750; d) A. Swidan, C. L. B. Macdonald, *Chem. Soc. Rev.* **2016**, *45*, 3883; e) Z. Niu, H. W. Gibson, *Chem. Rev.* **2009**, *109*, 6024–6049; f) B. Zheng, F. Wang, S. Dong, F. Huang, *Chem. Soc. Rev.* **2012**, *41*, 1621–1631; g) J. Li, D. Yim, W.-D. Jang, J. Yoon, *Chem. Soc. Rev.* **2017**, *46*, 2437–2458.
- [3] a) L. Liu, X. Wang, Q. Zhang, Q. Li, Y. Zhao, *CrystEngComm* **2013**, *15*, 841–844. b) D.-W. Lim, S. A. Chyun, M. P. Suh, *Angew. Chem.* **2014**, *126*, 7953–7956; *Angew. Chem. Int. Ed.* **2014**, *53*, 7819–7822. c) T.-H. Chen, A. Schneemann, R. A. Fischer, S. M. Cohen, *Dalton Trans.* **2016**, *45*, 3063–3069.
- [4] a) S. An, Q. Xu, Z. Ni, J. Hu, C. Peng, L. Zhai, Y. Guo, H. Liu, *Angew. Chem.* **2021**, *126*, 7953–7956; *Angew. Chem. Int. Ed.* **2021**, *60*, 9959–9963. b) S. An, C. Lu, Q. Xu, C. Lian, C. Peng, J. Hu, X. Zhuang, H. Liu, *ACS Energy Lett.* **2021**, *6*, 3496–3502.
- [5] N. A. Al-Jallal, A. A. Al-Kahtani, and A. A. El-Azary, *J. Phys. Chem. A* **2005**, *109*, 3694–3703.
- [6] a) J. Luo, J.-W. Wang, J.-H. Zhang, S. Lai, D.-C. Zhong, D.-C. *CrystEngComm* **2018**, *20*, 5884–5898; b) R.-B. Lin, Y.-B. He, P. Li, H.-L. Wang, W. Zhou, B. Chen, *Chem. Soc. Rev.* **2019**, *48*, 1362–1389; c) I. Hisaki, C. Xin, K. Takahashi, T. Nakamura, *Angew. Chem.* **2019**, *131*, 11278–11288; *Angew. Chem. Int. Ed.* **2019**, *58*, 11160–11170; d) B. Wang, R.-B. Lin, Z.-J. Zhang, S.-C. Xiang, B. Chen, *J. Am. Chem. Soc.* **2020**, *142*, 14399–14416; e) P.-H. Li, M. R. Ryder, J. F. Stoddart, *Acc. Mater. Res.* **2020**, *1*, 77–87. X. Song, Y. Wang, C. Wang, D. Wang, G. Zhuang, K. O. Kirlikovali, P. Li, O. K. Farha, *J. Am. Chem. Soc.* **2022**, *144*, 10663–10687.
- [7] a) G. G. Talanova, N. S. A. Elkarim, V. S. Talanov, R. E. Hanes, Jr., H.-S. Hwang, R. A. Bartsch, R. D. Rogers, *J. Am. Chem. Soc.* **1999**, *121*, 11281–11290; b) J. C. Bryan, *Acta Crystallogr. Sect. C* **2001**, *57*, 1359–1360.
- [8] a) I. Hisaki, S. Nakagawa, N. Tohnai, M. Miyata, *Angew. Chem.* **2015**, *127*, 3051–3055; *Angew. Chem. Int. Ed.* **2015**, *45*, 3008–3012; b) I. Hisaki, S. Nakagawa, N. Ikenaka, Y. Imamura, M. Katouda, M. Tashiro, H. Tsuchida, T. Ogoshi, H. Sato, N. Tohnai, M. Miyata, *J. Am. Chem. Soc.* **2016**, *138*, 6617–6628; c) I. Hisaki, Y. Suzuki, E. Gomez, Q. Ji, N. Tohnai, T. Nakamura, A. Douhal, *J. Am. Chem. Soc.* **2019**, *141*, 2111–2121.
- [9] X. Chen, K. Takahashi, K. Kokado, T. Nakamura, I. Hisaki, *Mater. Adv.* **2021**, *2*, 5639–5644.
- [10] Deposition Numbers 2192468 (for **3CT18C6-I**) and 2192469 (for **3CT18C6-Ia**) contain the supplementary crystallographic data for this paper. These data are provided free of charge by the joint Cambridge Crystallographic Data Centre and Fachinformationszentrum Karlsruhe Access Structures service.
- [11] a) P. v. d. Sluis, A. L. Spek, *Acta Crystallogr. Sect. A* **1990**, *46*, 194; b) A. L. Spek, *Acta Crystallogr. Sect. D* **2009**, *65*, 148–155.
- [12] A. Karmakar, R. Illathvalappil, B. Anothumakkool, A. Sen, P. Samanta, A. V. Desai, S. Kurungot, S. K. Ghosh, *Angew. Chem. Int. Ed.* **2016**, *55*, 10667–10671.
- [13] S. C. Pal, D. Mukherjee, R. Sahoo, S. Mondal, M. C. Das, *ACS Energy Lett.* **2021**, *6*, 4431–4453.

- [14] L. Jiménez-García, A. Kaltbeitzel, W. Pisula, J. S. Gutmann, M. Klapper, K. Mullen, *Angew. Chem.* **2009**, *121*, 10135-10138; *Angew. Chem. Int. Ed.* **2009**, *48*, 9951-9953.
- [15] W. Yang, F. Yang, T.-L. Hu, S. C. King, H. Wang, H. Wu, W. Zhou, J.-R. Li, H. D. Arman, B. Chen, *Cryst. Growth Des.* **2016**, *16*, 5831-5835.
- [16] Z.-B. Sun, Y.-L. Li, X.-H. Zhang, Z.-F. Li, B. Xiao, G. Li, *New J. Chem.* **2019**, *43*, 10637-10644.
- [17] G. L. Xing, T. T. Yan, S. Das, S. L. Qiu, T. Ben, *Angew. Chem.* **2018**, *130*, 5443-5447; *Angew. Chem. Int. Ed.* **2018**, *57*, 5345-5349.
- [18] Q. Yang, Y. Wang, Y. Shang, J. Du, J. Yin, D. Liu, X. Kang, R. Wang, D. Sun, J. Jiang, *Cryst. Growth Des.* **2020**, *20*, 3456-3465.
- [19] N.-N. Ji, Z.-Q. Shi, X.-X. Xie, G. Li, *CrystEngComm* **2020**, *22*, 8161-8165.
- [20] D.W. Lim, H. Kitagawa, *Chem. Soc. Rev.* **2021**, *50*, 6349-6368.

Entry for the Table of Contents



A porous hydrogen-bonded framework (HOF) was constructed from 18-crown-6-ether (18C6) derivative. Although a 18C6 macrocycle is flexible and has many possible conformations, directional intermolecular hydrogen-bonds of dicarboxy-*o*-terphenyl modules in the periphery of 18C6 allowed to form rigid HOF with 1D channels with bottleneck composed of 18C6 rings. The wet HOF shows proton conductivity ($1.12 \times 10^{-7} \text{ S cm}^{-1}$) through Grotthuss mechanism ($E_a = 0.27 \text{ eV}$) under 98%RH.

Institute and/or researcher Twitter usernames: @HisakiLab